ACS APPLIED POLYMER MATERIALS

Article

Cite This: ACS Appl. Polym. Mater. 2019, 1, 1778−1786

pubs.acs.org/acsapm

Isoindigo-Based Binary Polymer Blends for Solution-Processing of Semiconducting Nanofiber Networks

Aristide Gumyusenge,[†] Xuyi Luo,[†] Hongyi Zhang,[†] Gregory M. Pitch,[‡] Alexander L. Ayzner,[‡] and Jianguo Mei*,[†]

[†]Department of Chemistry, Purdue University, 560 Oval Drive, West Lafayette, Indiana 47907, United States

[‡]Department of Chemistry and Biochemistry, University of California Santa Cruz, 1156 High Street, Santa Cruz, California 95064, United States

Supporting Information

ABSTRACT: Molecular self-assembly in isoindigo-based binary polymer blends as a novel platform for facile and robust formation of semiconducting nanofibers is studied. We designed structurally complementary polymers to process all-semiconducting nanocomposites. The selection of the tie-polymer for nucleation and nanofiber formation was probed by tuning crystallinity via side chain engineering. Morphology studies revealed that the crystallinity and the scale-like morphology of the tie-polymer play a crucial role in making long and well stacked nanofiber networks. The optimized blends could be solution-processed into nanotailored semiconducting thin films with no postprocessing steps required. The nanofiber formation in thin films further led to lowered elastic moduli and glass transition but higher crack-on-set strain as well as excellent charge transport properties. The formed nanofibers could also be aligned via a blade-directed shearing method to fabricate organic field-effect transistor devices. Our blending strategy shows to be a promising facile route for processing flexible and stretchable organic semiconducting thin films.

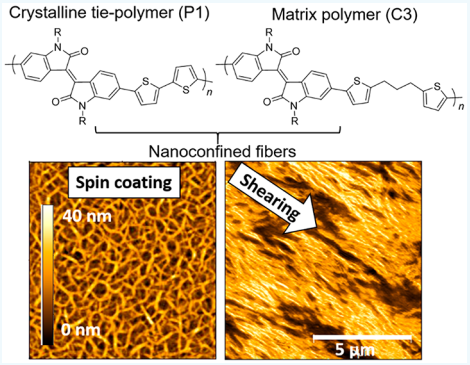

KEYWORDS: *polymer blends, semiconducting nanofibers, organic field-effect transistors, stretchable electronics, solution processing*

INTRODUCTION

Tough yet ductile organic thin films that can mechanically conform to flexible substrates are attractive for their applications in organic electronics.[1−5] Engineering approaches have been utilized to tune the mechanical properties of electronic devices by reducing their thickness.[6,7] The introduction of buckles and wavy structures has served as a tool to significantly increase the devices' conformability, and arrays that can withstand mechanical deformations have been realized.[2] Achieving the intrinsic stretchability for organic semiconductors is challenging, mainly because the needed π-conjugation in most semiconducting materials makes them rigid.[8] Both molecular and materials design approaches have been utilized to attain stretchable conjugated polymer thin films, such as using nanocomposites, backbone and side chain engineering, as well as cross-linking.[9−13] In the nanocomposite approach, self-assembled semiconducting polymers have gained remarkable attention owing to their ability to yield mechanically tough and flexible thin films, specifically when assembled into nanowires, without sacrificing the desired electronic properties.[14−20] In addition, nanowire-based electronic devices have been demonstrated and showed high electronic performance due to the aligned morphologies in fibers.[18,21,22] One notable approach to attain semiconductor self-assembly reported by Bao et al. has been the use of the nanoconfinement effect to assemble conjugated polymers into nanocomposites.[9,23] At the nanoscale level, mechanical properties of conjugated polymers can be tuned as polymer chains demonstrate local freedom within the confined surroundings. Devices able to stretch up to 100% could be realized when nanofiber-based organic films were utilized.

The nanofibers formation in conjugated polymers is often achieved via cross-linking or physical blending with insulating hosts. Conjugated polymers have shown to self-assemble into long-range aggregates mostly because of induced segmental motion of the conjugated polymer chains within the host matrices.[22,24−28] As a result of molecularly structural incompatibility, phase segregation between the two polymer components commonly occurs. By inducing the dual layer formation and the reorganization of the functional material at substrate's surface, oftentimes these binary systems yield improved electrical performances.[26,29,30] Notably, this strategy requires the use of large amounts of the insulating hosts, making it a less attractive route for practical applications. In cases where one might need to access the deposited

Received: April 6, 2019
Accepted: May 30, 2019
Published: June 17, 2019

DOI: 10.1021/acsapm.9b00321
ACS Appl. Polym. Mater. 2019, 1, 1778−1786

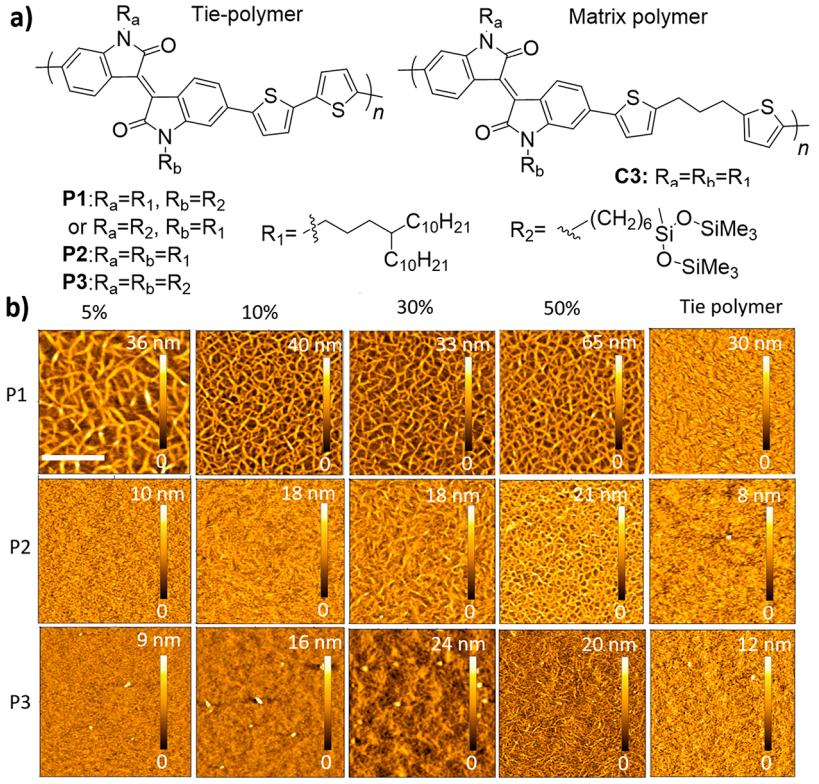

Figure 1. (a) Molecular design for tie-polymers (P1, P2, and P3) and matrix polymer (C3). Side chain engineering is used to tune the tie-polymer's crystallinity and aggregation. (b) AFM height images demonstrating the formation of polymer nanofibers in C3-based blends with varying blending ratios with the tie-polymers. The scale bar is 4 μm.

semiconducting layer, additional steps to remove the inactive component would be required.

A robust way to process semiconducting nanofiber networks into readily usable thin films would be the use of all-semiconducting components for fiber formation. Our research group has recently demonstrated the concept of complementary semiconducting polymer blends (*c*-SPBs).[31−34] In principle, a matrix polymer is designed to be highly flexible and serve as a blending medium for a small portion of a fully conjugated analogue. By introducing flexible conjugation break spacers (CBS), the main chain rigidity can be intentionally interrupted. To restore efficient charge transport, a small portion of the fully conjugated polymer is added to serve as tie-chains between the crystalline domains of the matrix polymer. This blending system of two structurally similar (i.e., complementary) polymers has been shown to be a robust way to improve polymer processability and yield excellent thin-film morphology as well as efficient charge transport in organic field-effect transistors (OFETs). By using a semiconducting matrix polymer—as opposed to using large percentages of insulating matrices—efficient active material density is achieved in *c*-SPBs. As a result of the lack of phase separation, however, the previously studied diketopyrrolopyrrole (DPP)-based binary systems did not exhibit the formation of self-assembled nanocomposites. Instead, the blend films showed uniform morphologies with no observable phase separation.[31,32] In addition, from recent reports on the formation of polymer nanofibers, this self-assembly feature seems to be observable for the fully conjugated polymers that readily form large crystalline aggregates, a behavior which was not observed in DPP-polymers.[21,23,25,26] The role of the tie-chain crystallinity during the nanofiber formation would thus be of interest, especially because there seems to be a lack of a guideline on which polymer combinations would lead to nanofiber self-assembly.

Here we report on the tie-polymer selection based on crystallinity and aggregation behavior in isoindigo-based binary polymer blends for nanofiber network formation. We design a matrix polymer that is structurally complementary to the tie-polymer to attain all-semiconducting blends. We use morphology analysis to probe the nanofiber formation process using three different tie-polymers in their blends with the newly designed matrix. We found that the more crystalline the nucleation sites (i.e., the tie-chains), the easier the formation of the nanofibers. The optimized binary blends showed the formation of long nanowires when as little as 5% of the fully conjugated polymer was used to form thin films. By increasing the blending ratio, the fiber interconnectivity could be increased for tailoring the nanofiber network. The binary blends containing only 10% of the tie-chain polymer showing excellent fiber interconnectivity could be readily solution-processed into thin films for transistor devices. The influence of the formation of nanofibers on the glass transition, crystallinity, mechanical properties, as well as charge transport properties under strain was then studied for solution-processed thin films. The formed nanofibers could further be disentangled using a blade-shearing method to fabricate transistor devices.

RESULTS AND DISCUSSION

Tie-Polymer Selection for Nanofiber Formation. In this study, isoindigo-based fully conjugated polymers (P1, P2, P3) were selected for nanofiber formation studies owing to the tendency of indigo-/isoindigo building blocks to aggregate and

DOI: 10.1021/acsapm.9b00321
ACS Appl. Polym. Mater. 2019, 1, 1778−1786

crystallize into long-range assemblies.[35,36] Additionally, in our previous studies, the differences in side chains flanking these tie-chains have been shown to lead to tunable crystallinities and aggregate morphologies.[36] We thus probe the influence of the crystallinity and morphology of the tie-polymer during nucleation and nanofiber growth in the semicrystalline host matrix (C3), in accordance with the complementary polymer blends model developed by our group.[31,37−39] We design C3 to serve as a structurally complementary matrix to form all-semiconducting blends for nanocomposite formation. Molecular structures of the fully conjugated polymers (P1, P2, P3) and the studied matrix polymer (C3) are shown in Figure 1a. Experimental details on the synthesis and characterization of the polymers can be found in the Supporting Information along with thin-film-processing details.

Morphology analyses were used to visualize the impact of the tie-polymer on self-assembly and fiber formation. By varying the blending ratio of the added tie-polymer in solution of C3, the fibers' length and interconnectivity could be tuned as seen from the corresponding atomic force microscopy (AFM) images (Figure 1b). From the AFM height morphology of the pure tie-polymers, P1 shows scale-like aggregates in comparison to the other two derivatives. In addition, X-ray studies on these polymers have previously revealed that the asymmetric side chains on P1 allow for mixed orientations and improved crystallinity in comparison to the symmetrical counterparts.[36] We could then predict that the more crystalline tie-polymer would aggregate better and serve as a more efficient nucleation site for the fiber growth.[40] When blended with C3, P1 exhibits abrupt formation of fiber networks in the spin-cast films when as little as 5% is used. A further increase in amount of P1 added leads to more stacked layers of the nanofiber networks. P2, which displays lower crystallinity and smaller aggregates from morphology analysis, could only form fibers when much higher amounts of nucleates were added (Figure 1b). It required as high as 30 wt % of P2 for fiber-like assemblies to be observed. Conversely, P3, the least crystalline of the three polymers, could not lead to nanofiber formation in its blends with C3. Long aggregates could be observed at higher percentage (>50 wt %), but no network formation could be observed. It was thus evident that to form a network of long nanofibers, the choice of the tie-chain was crucial in the studied isoindigo system. More crystalline tie-chains could serve as excellent nucleation sites for the semicrystalline matrix, and long-range nanofiber growth could be induced.

Charge Transport within Nanofiber Networks. The morphology behaviors of the three studied pairs allowed a comparative analysis on electrical properties in the blends. Because the three tie-polymers appear to induce different assemblies when blended with the matrix, we compare the resulting hole mobilities specifically to explore potential usage of the formed fibers for organic electronics. OFET devices were then fabricated by spin-casting the blend films with no further modification steps. The resulting hole mobilities are summarized in Table 1, and the corresponding transfer curves can be found in the Supporting Information along with the device fabrication details. Not surprisingly, the blends of P1 and C3 gave much better electronic properties compared to the other pairs. More intriguingly, even the blend containing only as little as 5% of P1 could reach an OFET mobility as high as 0.12 $cm^2/(V\ s)$ despite the large and randomly oriented fibers as observed from the AFM images. The ability of the nanofiber-based films to achieve excellent electronic properties without exhibiting detrimental grain boundaries could thus be attributed to the fact we use all-semiconducting components in the blends. In the case of P2 and P3 blends, these tie-polymers were not only unable to induce long-range crystallization in the blend films but also they could not perform as efficient bridging tie-chains for charge transport. The average charge mobilities for these parent tie-polymers were measured to be 0.12 and 0.11 $cm^2/(V\ s)$ for P2 and P3, respectively, whereas P1 showed much higher mobilities (~2.85 $cm^2/(V\ s)$) (Figure S3). We then carried out a series of studies on the P1-based blends to explore their potential applications in organic electronics, especially for the ratios containing large amounts of the easily processable C3.

Table 1. Comparison of Hole Mobility in OFET Devices Based on Blends of C3 with Increasing wt % of the Studied Tie-Polymers

tie-polymer % in blend	P1 (avg, max μ_h ($cm^2/(V\ s)$))	P2 (avg, max μ_h ($cm^2/(V\ s)$))	P3 (avg, max (μ_h $cm^2/(V\ s)$))
5%	0.090, 0.11	0.013, 0.055	0.0023, 0.0037
10%	0.096, 0.12	0.015, 0.064	0.0031, 0.0045
30%	0.15, 0.30	0.021, 0.065	0.0037, 0.0052
50%	0.22, 0.37	0.032, 0.070	0.0065, 0.010
70%	0.51, 0.72	0.08, 0.093	0.010, 0.012

Crystallization Behaviors in Nanofiber Networks. Because the blending of P1 and C3 revealed to lead to drastic changes in thin-film morphology, we carried out a series of studies on polymer chain behaviors within the formed networks. First, from the UV−vis absorption spectra, we observed that nanofibers are not simply from the aggregation of P1 within the matrix polymer. By increasing the blending ratio from 5% up to 90% P1, the UV−vis absorption spectra show no red-shift in the peaks' maxima, which would indicate long-range aggregation of P1 (Figure 2a,b). This kind of long-range aggregation was observed when we compared our blending system to polystyrene blends of P1 (Figure S4). When blended with polystyrene, the tie-polymer could only phase separate and aggregate into large fiber-like domains, resulting into a large (~20 nm) red-shift in the *0−0* vibronic peak. For C3 blends, instead of aggregation of P1 and red-shifting in absorption, the *0−0* peak intensity appeared to increase with increasing amounts of P1 added (Figure 2c), which agreed with the stacking of fiber networks revealed by the AFM images. We could thus deduce that, upon blending, chains of P1 serve as nucleation sites for the complementary matrix, resulting in the growth of stacks of nanofibers. This simultaneous crystallization of the binary components into nanofibers was further revealed to induce excellent chain packing within the formed fibers as seen from the grazing incidence X-ray diffraction (GIXRD) analysis (Figure 2d,e). In addition, the diffraction patterns of the blend films exhibited a broad ring-like Bragg reflection around q = 1.5 $Å^{-1}$, in comparison to the parent C3 and P1, suggesting the formation of isotropic domains within the thin film, which we associated with the stacking nature of the formed fibers. However, both lamellar packing and $\pi-\pi$ stacking could be retained, and new packing distances were adopted within the fibers (Figure 2e,f). It is also worth noting that the isotropic character of the $\pi-\pi$ stacking peak is most likely due to polymer chains packing well

DOI: 10.1021/acsapm.9b00321
ACS Appl. Polym. Mater. 2019, 1, 1778−1786

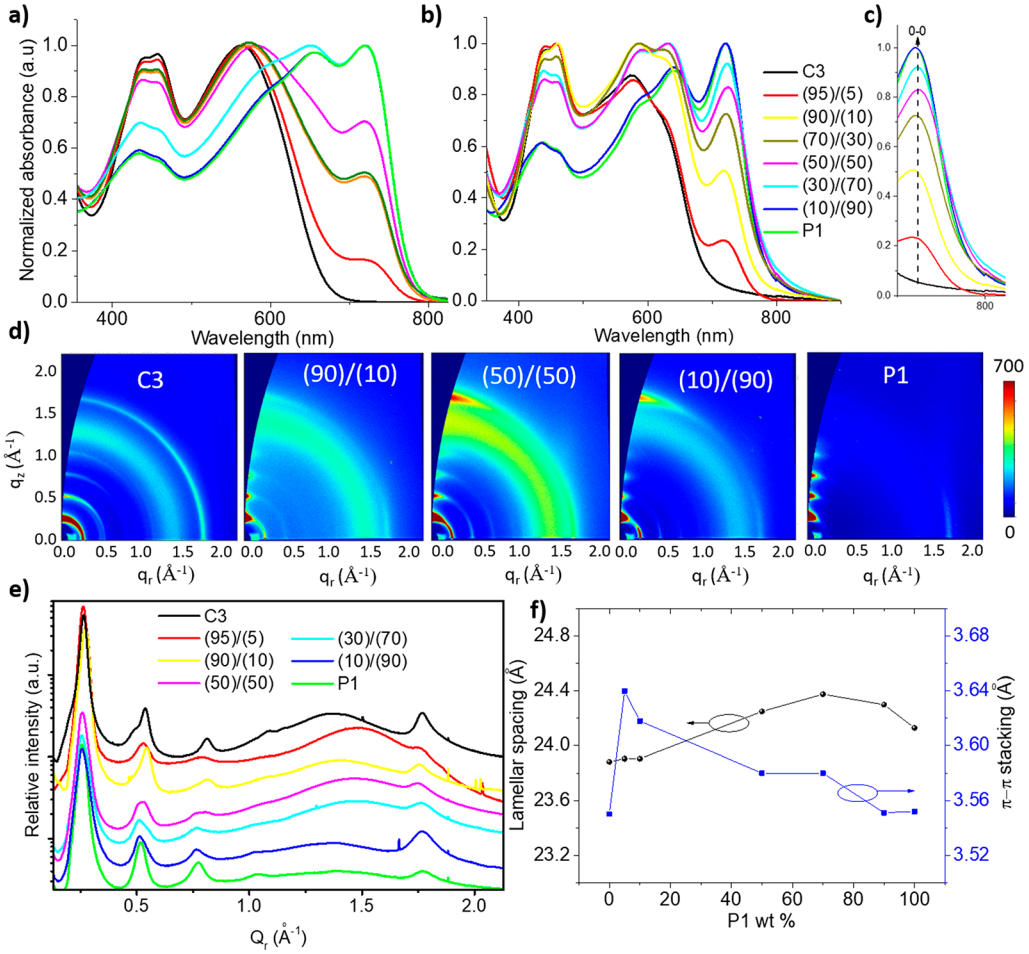

Figure 2. UV−vis absorption spectra of (a) solution and (b) thin films with varying blending ratios of C3 and P1. (c) Evolution of the *0−0* vibronic peak upon blending. (d) GIXRD diffraction patterns and (e) the corresponding orientationally averaged $I(q)$ vs q plots of solution-processed thin films with different blending ratios of (C3)/(P1) revealing the change in crystallinity upon formation of nanofibers. The *y*-axes were offset for clarity. (f) Extracted peak positions for $\pi-\pi$ and lamellar packing in the blend films.

within the formed fibers, which are oriented in all directions. This ability of the nanofiber films to retain excellent packing, the most efficient pathway for charge transport, would thus make this system suitable for electronic applications.

Impact of Nanofiber Formation on Thin-Film Glass Transition. Given the morphological behavior of the binary blends, we envisioned the nanofiber network formation to have an impact on the thin-film physical properties, notably the glass transition temperature (T_g). The formation of nanofibers has been utilized in tuning the polymer's physical behavior via what is known as the nanoconfinement effect.[23] When confined to nanoscale environments, the polymer chain's segmental motion has been shown to differ from that of the bulk state, and this behavior has been associated with a reduced neighboring effect leading to lowered T_g.[41−44] This softening effect by nanoconfinement has thus been utilized to design highly flexible and stretchable thin films for organic electronics.[9,23] T_g extrapolation of polymer thin films using UV−vis absorption was recently reported by Root et al. and was herein utilized for the studied blend system as a straightforward tool to study the influence of the observed solid-state morphologies on glass transition.[45] In this technique, polymer thin films are annealed (or quenched) to different temperatures, and the corresponding UV−vis absorption spectra are obtained at each temperature. Root and co-workers could show, using molecular dynamics calculations, that when the annealing temperature approaches the glass transition, abrupt changes in the absorption occur due to molecular chain rearrangements. This change in absorption could then be quantified using a parameter termed "the deviation metric". The temperature at which the deviation metric starts to increase correlates to the glass transition. This thin-film-based method was further validated for a wide scope of semi/crystalline semiconducting polymers. We thus employed this technique to evaluate the impact of nanofiber formation in thin films on the resulting glassiness. The experimental details on the T_g measurements can be found in the Supporting Information as well as the temperature dependent absorption spectra used for T_g calculation. Figure 3a−c show the extracted T_g values for P1 and its 10% blend in C3 using the solid-state UV−vis absorption method. P1, whose solid-state morphology revealed large crystalline aggregates, showed a glass transition at −60 °C. Similar results were also obtained using rheology measurements (Figure S6).[46] When blended with C3 ($T_g \approx -46$ °C), the glass transition temperature could be detected at −75 °C, suggesting that the film becomes less rigid after blending and takes much lower quenching temperatures to vitrify. It could thus be concluded that because of the formation of the nanofiber network, the glass transition temperature of the thin films is much lower for

DOI: 10.1021/acsapm.9b00321
ACS Appl. Polym. Mater. 2019, 1, 1778−1786

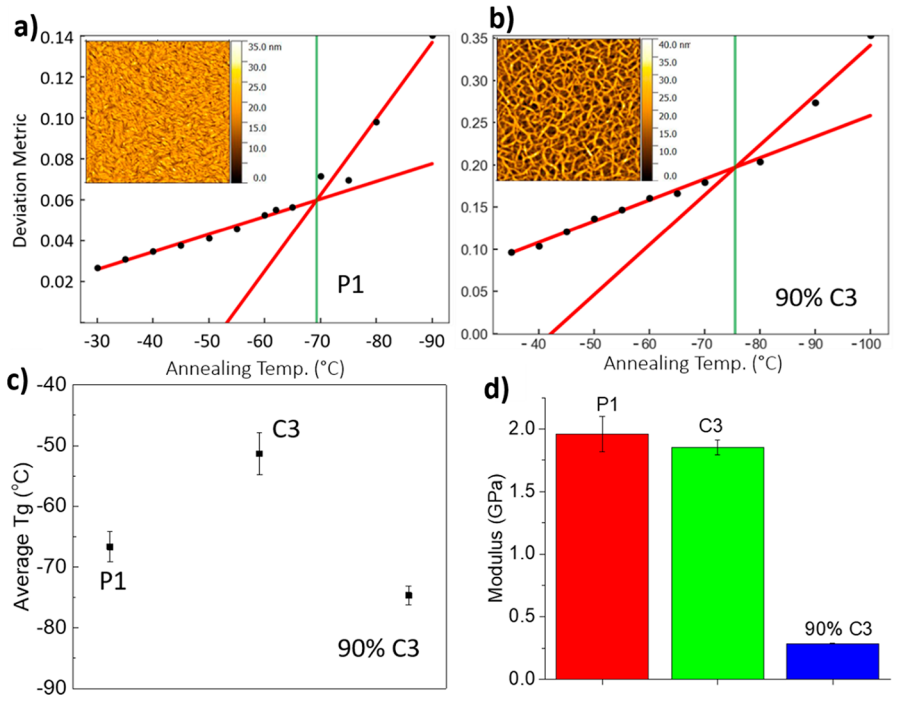

Figure 3. Glass transition comparison between aggregated polymer films and nanotailored blend films. Extracted T_g values from temperature dependent UV−vis absorption spectra for (a) P1 and (b) its blend films. Comparison of (c) T_g and (d) Young modulus modulation in thin films by the nanoconfinement effect. The nanofiber formation leads to more ductile films.

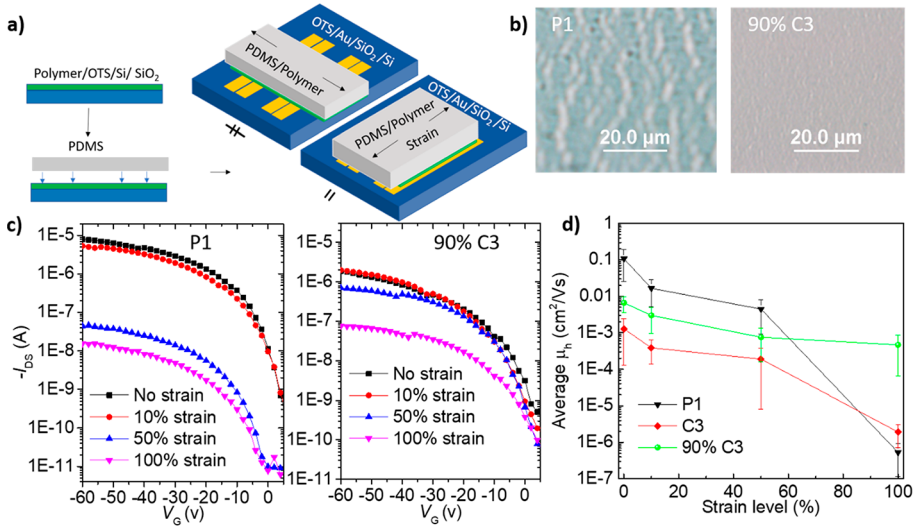

Figure 4. (a) Illustration of the soft-contact lamination method for OFET devices' stretchability analysis. (b) Micrographs of thin films stretched up to 100% with noticeable breakdown in P1 and only minor imprints in the C3 blend films. (c) Change in source−drain current as a function of applied strain perpendicular to the channel (‡). (d) Average hole mobility under applied strain.

the C3-based blends. The polymer chains confined into nanowires could form thin films with improved ductility.

This loss in film ridigity for C3/P1 blends could also translate into improved mechanical properties of the blend films studied using the buckling method.[47] We compared the mechanical behavior of the blend film to that of the pure components to probe the influence of fibers on thin-film ductility. By transferring the spin-cast films onto prestrained PDMS substrates, buckles could be formed and used to extract the films' elastic moduli. Figure S7 illustrates the buckling method, and experimental details as well as the used optical images can be found in the Supporting Information. The elastic modulus was extracted using eq 1

$$E_f \approx 3E_s \times \left(\frac{\lambda}{2\pi h}\right)^3 \quad (1)$$

where E_f is the film modulus, E_s the measured substrate's modulus, λ is the buckle's periodicity extracted from optical images, and h is the film thickness, which was measured by AFM to be around 100 nm. Upon buckling, pure P1 showed an elastic modulus of ∼0.5 GPa (in good agreement with reported values).[36] The pure semicrystalline isoindigo-based matrix also showed modulus to the same order, as these

DOI: 10.1021/acsapm.9b00321
ACS Appl. Polym. Mater. 2019, 1, 1778−1786

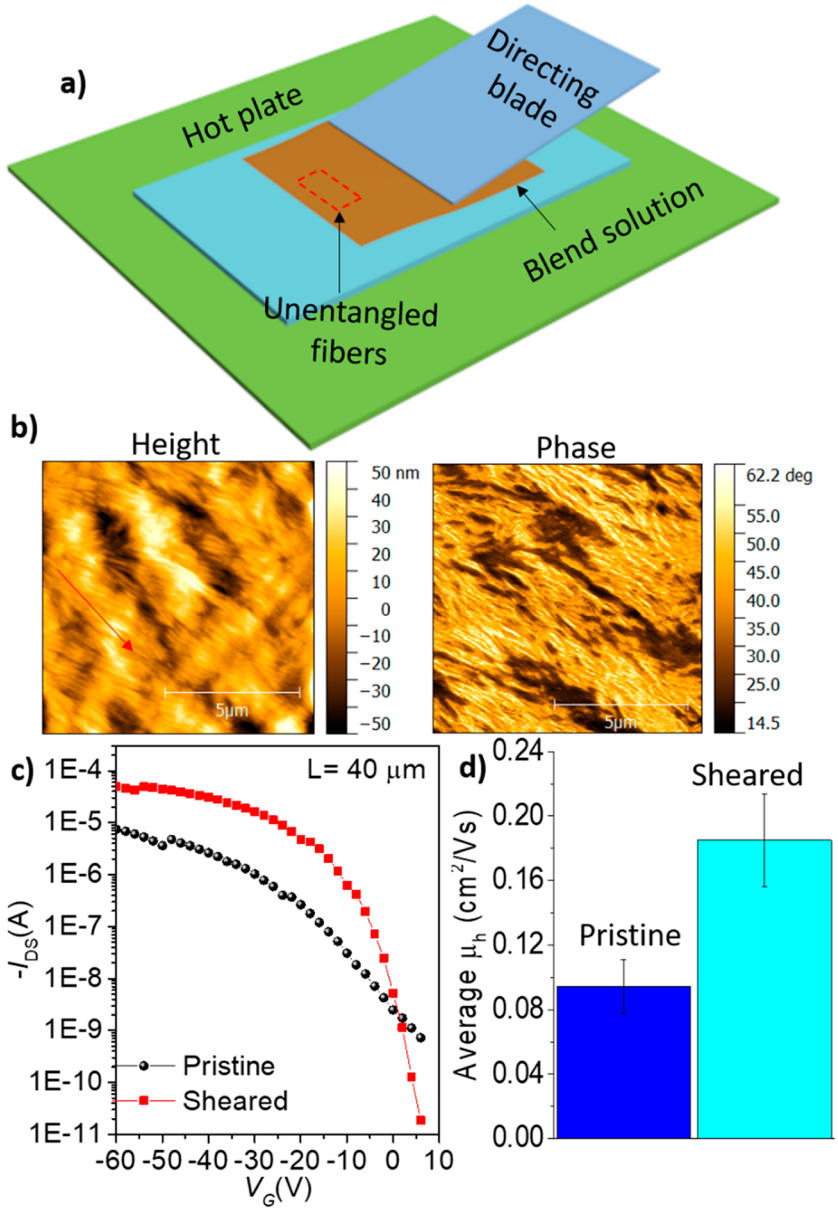

Figure 5. (a) Demonstration of nanofiber disentanglement by the blade-shearing method. A directing blade is used to align polymer chains in the shearing direction. (b) AFM height and phase images of the sheared film showing aligned fibers. (c) Output current and (d) hole mobility comparison for OFET devices based on spin-cast and sheared C3/P1 blend films.

polymers tend to be soft materials. The blends containing 10% of P1 displaying the formation of a nanofiber network showed a significant decrease, as much as 10-fold, in the modulus (Figure 3d). This tunability of the thin film's mechanical properties in the binary and complementary system could again be attributed to the formation of a nanofiber network, leading to much more ductile thin films in agreement with T_g and crystallinity results.

Crack-on-Set Strain and OFET Characterization. Studies were carried out to demonstrate the potential applicability of the formed nanofiber networks for stretchable electronics. The crack-on-set strain of pure P1-based films was compared to that of the films based on self-assembled blends using the previously reported soft-contact lamination method.[48] The ability of the polymer thin films to retain original electronic performance after 10, 50, and 100% stretching was evaluated on OFET devices. Figure 4a shows the illustration of the soft-contact lamination using PDMS. The lamination of the PDMS/polymer assembly was done both parallel (∥) and perpendicular (‡) to the device channel. Figure 4b shows the optical micrographs demonstrating the formation of microcracks in films of P1 in comparison to the nanofiber-forming 90% C3 blend at 100% strain. Figure 4c shows the OFET devices' source−drain current as a function of applied strain for the devices based on the perpendicular lamination. The experimental details on the device fabrication and characterization can be found in the Supporting Information. Optical micrographs indicating the formation of cracks under different strains are shown in Figure S8. OFET performances of devices fabricated by parallel lamination are also summarized in Table S1, and characteristic transfer curves of studied devices under perpendicular lamination are shown in Figure S9.

P1 and C3 showed an average hole mobility around 0.1 and 0.002 $cm^2/(V\ s)$, respectively, with no strain applied, whereas

DOI: 10.1021/acsapm.9b00321
ACS Appl. Polym. Mater. 2019, 1, 1778−1786

the nanofiber-based films showed performances around 0.02 cm^2 /(V s) for the 90% C3. Despite lower OFET performances obtained after soft-contact lamination in comparison to spin-cast films, most likely because of surface defects introduced during the transfer, the studied method proved to be a facile way to evaluate the polymer thin films' stretchability.[48] Upon 10% stretching, the performance thin-film transistor devices based on pure P1 and C3 decreased by an order of magnitude. The nanofiber-based films, on the contrary, retained up to 50% of their electrical performance, even up to 100% stretching (Figure 4d). This loss in electronic performance in the case of pure polymers was associated with formed cracks in the films, as confirmed by the optical images (Figure S8). The blends that formed fibers showed excellent mechanical stability with a crack-on-set higher than 80%. This mechanical stability could be explained by the previously discussed nanoconfinement effect that leads to improved thin-film ductility when nanofibers are formed. We thus conclude that the formed nanofiber networks improved the mechanical stability of the thin films consisting of the isoindigo binary blends and the transistor devices made therefrom. Despite modest performances by the currently studied blends, this kind of conformability and electrical stability under strain is desired for flexible and stretchable device applications.

Uniaxial Alignment of the Nanowires. This was further studied to demonstrate potential uses of the formed fibers for applications requiring chain orientation. The impact of alignment on charge carrier properties was also studied. Commonly, in the case of desired uniaxial alignment, aging and/or UV curing have been utilized to align semiconducting polymers in one direction.[40,49,50] The blend system studied here could be used for solution shearing, and alignment could be achieved without any further growth and/or aging steps required as the fibers showed to form upon solution-casting. This would serve as a new platform to facilitate the fabrication of electronic devices that require semiconductor alignment. Figure 5a illustrates the shearing method using a blade to direct the blend solution to attain highly aligned fibers upon solvent evaporation. AFM images of the aligned film revealed that the nanofibers could be disentangled along the shearing direction (Figure 5b). This kind of disentanglement behavior would find applications in manufacturing techniques such slot-die and blade coating.

The sheared films were also used to fabricate OFET devices to further probe the applicability of this fabrication route in organic electronics. Figure 5c,d shows the comparison of output current and hole mobility, respectively, between unaligned films and sheared films. Corresponding transfer curves are shown in Figure S10. Upon shearing, the charge carrier mobility could be doubled, suggesting that the alignment does not greatly perturb the polymer packing, at the nanoscale level, and did not introduce a large grain boundary effect within the film.[51] We could then safely conclude that preferred self-assembly is attained from blending and not the shearing itself. Hole mobilities reaching 0.25 cm^2/(V s) could be attained via simple blade shearing, making this blending system an attractive system for solution-based device fabrication. Additionally, because the nanowires are predominantly composed of the matrix polymer, this blend system also finds applications in melt-processing and/or welding of the nanofibers.[52,53] The matrix polymer's melting temperatures can readily be tuned via side chain engineering as well as the conjugation break spacer length,[31,34,39] making the studied binary blends good candidates for forming easily processable and aligned nanofibers.

CONCLUSIONS

To summarize, we have demonstrated the formation of nanofibers in isoindigo semiconducting polymer binary blends. Tie-polymer selection was used to achieve longer and well-interconnected nanowires via side chain engineering. The nanofiber-based films demonstrated lower glass transition temperatures, lower rigidity, and excellent mechanical properties in comparison to the pure polymers. The ductile films also showed excellent charge transport properties, thus demonstrating their relevance in flexible and stretchable electronics. We expect this isoindigo-based blending system to serve as a facile platform to achieve highly ductile, yet semiconducting thin films for electronics applications. Because the fibers contain mainly the semiconducting matrix polymer, we intend to conduct further studies on matrix engineering for the melt-processing of the nanowires.

ASSOCIATED CONTENT

Supporting Information

The Supporting Information is available free of charge on the ACS Publications website at DOI: 10.1021/acsapm.9b00321.

Detailed physical characterization experiments as well as supporting figures and tables (PDF)

AUTHOR INFORMATION

Corresponding Author

*E-mail: jgmei@purdue.edu.

ORCID

Alexander L. Ayzner: 0000-0002-6549-4721

Jianguo Mei: 0000-0002-5743-2715

Notes

The authors declare no competing financial interest.

ACKNOWLEDGMENTS

The authors appreciate the financial support from the National Science Foundation (Award number: 1653909) and the startup fund from Purdue University. Dr. Xikang Zhao provided the materials for the initial tests. Renxuan Xie and Prof. Enrique Gomez performed the rheology measurements. GIXRD measurements were taken at the Stanford Synchrotron Radiation Laboratory, a national user facility operated by Stanford University on behalf of the U.S. Department of Energy, Office of Basic Energy Sciences.

REFERENCES

(1) Hammock, M. L.; Chortos, A.; Tee, B. C. K.; Tok, J. B. H.; Bao, Z. 25th Anniversary Article: The Evolution of Electronic Skin (E-Skin): A Brief History, Design Considerations, and Recent Progress. *Adv. Mater.* **2013**, *25*, 5997−6038.

(2) Kaltenbrunner, M.; Sekitani, T.; Reeder, J.; Yokota, T.; Kuribara, K.; Tokuhara, T.; Drack, M.; Schwodiauer, R.; Graz, I.; Bauer-Gogonea, S.; Bauer, S.; Someya, T. An ultra-lightweight design for imperceptible plastic electronics. *Nature* **2013**, *499*, 458−463.

(3) Reeder, J.; Kaltenbrunner, M.; Ware, T.; Arreaga-Salas, D.; Avendano-Bolivar, A.; Yokota, T.; Inoue, Y.; Sekino, M.; Voit, W.; Sekitani, T.; Someya, T. Mechanically Adaptive Organic Transistors for Implantable Electronics. *Adv. Mater.* **2014**, *26*, 4967−4973.

(4) Rogers, J. A.; Someya, T.; Huang, Y. Materials and Mechanics for Stretchable Electronics. *Science* **2010**, *327*, 1603−1607.

DOI: 10.1021/acsapm.9b00321
ACS Appl. Polym. Mater. 2019, 1, 1778−1786

(5) Sekitani, T.; Noguchi, Y.; Hata, K.; Fukushima, T.; Aida, T.; Someya, T. A Rubberlike Stretchable Active Matrix Using Elastic Conductors. *Science* **2008**, *321*, 1468−1472.
(6) Sekitani, T.; Zschieschang, U.; Klauk, H.; Someya, T. Flexible organic transistors and circuits with extreme bending stability. *Nat. Mater.* **2010**, *9*, 1015−1022.
(7) Suo, Z.; Ma, E. Y.; Gleskova, H.; Wagner, S. Mechanics of rollable and foldable film-on-foil electronics. *Appl. Phys. Lett.* **1999**, *74*, 1177−1179.
(8) Wang, C.; Dong, H.; Hu, W.; Liu, Y.; Zhu, D. Semiconducting π-Conjugated Systems in Field-Effect Transistors: A Material Odyssey of Organic Electronics. *Chem. Rev.* **2012**, *112*, 2208−2267.
(9) Wang, Y.; Zhu, C.; Pfattner, R.; Yan, H.; Jin, L.; Chen, S.; Molina-Lopez, F.; Lissel, F.; Liu, J.; Rabiah, N. I.; Chen, Z.; Chung, J. W.; Linder, C.; Toney, M. F.; Murmann, B.; Bao, Z. A highly stretchable, transparent, and conductive polymer. *Sci. Adv.* **2017**, *3*, e1602076.
(10) Wang, G.-J. N.; Shaw, L.; Xu, J.; Kurosawa, T.; Schroeder, B. C.; Oh, J. Y.; Benight, S. J.; Bao, Z. Inducing Elasticity through Oligo-Siloxane Crosslinks for Intrinsically Stretchable Semiconducting Polymers. *Adv. Funct. Mater.* **2016**, *26*, 7254−7262.
(11) Lipomi, D. J.; Bao, Z. Stretchable and ultraflexible organic electronics. *MRS Bull.* **2017**, *42*, 93−97.
(12) Qian, Y.; Zhang, X.; Xie, L.; Qi, D.; Chandran, B. K.; Chen, X.; Huang, W. Stretchable Organic Semiconductor Devices. *Adv. Mater.* **2016**, *28*, 9243−9265.
(13) Rao, Y.-L.; Chortos, A.; Pfattner, R.; Lissel, F.; Chiu, Y.-C.; Feig, V.; Xu, J.; Kurosawa, T.; Gu, X.; Wang, C.; He, M.; Chung, J. W.; Bao, Z. Stretchable Self-Healing Polymeric Dielectrics Cross-Linked Through Metal−Ligand Coordination. *J. Am. Chem. Soc.* **2016**, *138*, 6020−6027.
(14) Heeger, A. J. Semiconducting and metallic polymers: the fourth generation of polymeric materials. *Synth. Met.* **2001**, *125*, 23−42.
(15) Hoeben, F. J. M.; Jonkheijm, P.; Meijer, E. W.; Schenning, A. P. H. J. About Supramolecular Assemblies of π-Conjugated Systems. *Chem. Rev.* **2005**, *105*, 1491−1546.
(16) Li, J.; Ma, P. C.; Chow, W. S.; To, C. K.; Tang, B. Z.; Kim, J. K. Correlations between Percolation Threshold, Dispersion State, and Aspect Ratio of Carbon Nanotubes. *Adv. Funct. Mater.* **2007**, *17*, 3207−3215.
(17) Lipomi, D. J.; Vosgueritchian, M.; Tee, B. C. K.; Hellstrom, S. L.; Lee, J. A.; Fox, C. H.; Bao, Z. Skin-like pressure and strain sensors based on transparent elastic films of carbon nanotubes. *Nat. Nanotechnol.* **2011**, *6*, 788−792.
(18) Prasanthkumar, S.; Gopal, A.; Ajayaghosh, A. Self-Assembly of Thienylenevinylene Molecular Wires to Semiconducting Gels with Doped Metallic Conductivity. *J. Am. Chem. Soc.* **2010**, *132*, 13206−13207.
(19) Qin, L.; Park, S.; Huang, L.; Mirkin, C. A. On-Wire Lithography. *Science* **2005**, *309*, 113−115.
(20) Zang, L.; Che, Y.; Moore, J. S. One-Dimensional Self-Assembly of Planar π-Conjugated Molecules: Adaptable Building Blocks for Organic Nanodevices. *Acc. Chem. Res.* **2008**, *41*, 1596−1608.
(21) Briseno, A. L.; Mannsfeld, S. C. B.; Jenekhe, S. A.; Bao, Z.; Xia, Y. Introducing organic nanowire transistors. *Mater. Today* **2008**, *11*, 38−47.
(22) Luo, C.; Kyaw, A. K. K.; Perez, L. A.; Patel, S.; Wang, M.; Grimm, B.; Bazan, G. C.; Kramer, E. J.; Heeger, A. J. General Strategy for Self-Assembly of Highly Oriented Nanocrystalline Semiconducting Polymers with High Mobility. *Nano Lett.* **2014**, *14*, 2764−2771.
(23) Xu, J.; Wang, S.; Wang, G.-J. N.; Zhu, C.; Luo, S.; Jin, L.; Gu, X.; Chen, S.; Feig, V. R.; To, J. W. F.; Rondeau-Gagné, S.; Park, J.; Schroeder, B. C.; Lu, C.; Oh, J. Y.; Wang, Y.; Kim, Y.-H.; Yan, H.; Sinclair, R.; Zhou, D.; Xue, G.; Murmann, B.; Linder, C.; Cai, W.; Tok, J. B.-H.; Chung, J. W.; Bao, Z. Highly stretchable polymer semiconductor films through the nanoconfinement effect. *Science* **2017**, *355*, 59−64.
(24) Hopkins, A. R.; Reynolds, J. R. Crystallization Driven Formation of Conducting Polymer Networks in Polymer Blends. *Macromolecules* **2000**, *33*, 5221−5226.
(25) Lei, Y.; Deng, P.; Lin, M.; Zheng, X.; Zhu, F.; Ong, B. S. Enhancing Crystalline Structural Orders of Polymer Semiconductors for Efficient Charge Transport via Polymer-Matrix-Mediated Molecular Self-Assembly. *Adv. Mater.* **2016**, *28*, 6687−6694.
(26) Lei, Y.; Deng, P.; Li, J.; Lin, M.; Zhu, F.; Ng, T.-W.; Lee, C.-S.; Ong, B. S. Solution-Processed Donor-Acceptor Polymer Nanowire Network Semiconductors For High-Performance Field-Effect Transistors. *Sci. Rep.* **2016**, *6*, 24476.
(27) Liu, Y.; Zhao, J.; Li, Z.; Mu, C.; Ma, W.; Hu, H.; Jiang, K.; Lin, H.; Ade, H.; Yan, H. Aggregation and morphology control enables multiple cases of high-efficiency polymer solar cells. *Nat. Commun.* **2014**, *5*, 5293.
(28) Gumyusenge, A.; Tran, D. T.; Luo, X.; Pitch, G. M.; Zhao, Y.; Jenkins, K. A.; Dunn, T. J.; Ayzner, A. L.; Savoie, B. M.; Mei, J. Semiconducting polymer blends that exhibit stable charge transport at high temperatures. *Science* **2018**, *362*, 1131−1134.
(29) Qiu, L.; Lee, W. H.; Wang, X.; Kim, J. S.; Lim, J. A.; Kwak, D.; Lee, S.; Cho, K. Organic Thin-film Transistors Based on Polythiophene Nanowires Embedded in Insulating Polymer. *Adv. Mater.* **2009**, *21*, 1349−1353.
(30) Qiu, L.; Lim, J. A.; Wang, X.; Lee, W. H.; Hwang, M.; Cho, K. Versatile Use of Vertical-Phase-Separation-Induced Bilayer Structures in Organic Thin-Film Transistors. *Adv. Mater.* **2008**, *20*, 1141−1145.
(31) Zhao, X.; Zhao, Y.; Ge, Q.; Butrouna, K.; Diao, Y.; Graham, K. R.; Mei, J. Complementary Semiconducting Polymer Blends: The Influence of Conjugation-Break Spacer Length in Matrix Polymers. *Macromolecules* **2016**, *49*, 2601−2608.
(32) Zhao, Y.; Zhao, X.; Roders, M.; Gumyusenge, A.; Ayzner, A. L.; Mei, J. Melt-Processing of Complementary Semiconducting Polymer Blends for High Performance Organic Transistors. *Adv. Mater.* **2017**, *29*, 1605056.
(33) Zhao, Y.; Zhao, X.; Roders, M.; Qu, G.; Diao, Y.; Ayzner, A. L.; Mei, J. Complementary Semiconducting Polymer Blends for Efficient Charge Transport. *Chem. Mater.* **2015**, *27*, 7164−7170.
(34) Zhao, Y.; Zhao, X.; Zang, Y.; Di, C.-a.; Diao, Y.; Mei, J. Conjugation-Break Spacers in Semiconducting Polymers: Impact on Polymer Processability and Charge Transport Properties. *Macromolecules* **2015**, *48*, 2048−2053.
(35) Liu, C.; Xu, W.; Xue, Q.; Cai, P.; Ying, L.; Huang, F.; Cao, Y. Nanowires of indigo and isoindigo-based molecules with thermally removable groups. *Dyes Pigm.* **2016**, *125*, 54−63.
(36) Xue, G.; Zhao, X.; Qu, G.; Xu, T.; Gumyusenge, A.; Zhang, Z.; Zhao, Y.; Diao, Y.; Li, H.; Mei, J. Symmetry Breaking in Side Chains Leading to Mixed Orientations and Improved Charge Transport in Isoindigo-alt-Bithiophene Based Polymer Thin Films. *ACS Appl. Mater. Interfaces* **2017**, *9*, 25426−25433.
(37) Zhao, X.; Xue, G.; Qu, G.; Singhania, V.; Zhao, Y.; Butrouna, K.; Gumyusenge, A.; Diao, Y.; Graham, K. R.; Li, H.; Mei, J. Complementary Semiconducting Polymer Blends: Influence of Side Chains of Matrix Polymers. *Macromolecules* **2017**, *50*, 6202−6209.
(38) Zhao, Y.; Zhao, X.; Roders, M.; Qu, G.; Diao, Y.; Ayzner, A. L.; Mei, J. Complementary Semiconducting Polymer Blends for Efficient Charge Transport. *Chem. Mater.* **2015**, *27*, 7164−7170.
(39) Gumyusenge, A.; Zhao, X.; Zhao, Y.; Mei, J. Attaining Melt Processing of Complementary Semiconducting Polymer Blends at 130 °C via Side-Chain Engineering. *ACS Appl. Mater. Interfaces* **2018**, *10*, 4904−4909.
(40) Persson, N. E.; Chu, P.-H.; McBride, M.; Grover, M.; Reichmanis, E. Nucleation, Growth, and Alignment of Poly(3-hexylthiophene) Nanofibers for High-Performance OFETs. *Acc. Chem. Res.* **2017**, *50*, 932−942.
(41) Keddie, J. L.; Jones, R. A. L.; Cory, R. A. Size-Dependent Depression of the Glass Transition Temperature in Polymer Films. *EPL* **1994**, *27*, 59.
(42) Forrest, J. A.; Dalnoki-Veress, K.; Dutcher, J. R. Interface and chain confinement effects on the glass transition temperature of thin

DOI: 10.1021/acsapm.9b00321
ACS Appl. Polym. Mater. 2019, 1, 1778−1786

polymer films. *Phys. Rev. E: Stat. Phys., Plasmas, Fluids, Relat. Interdiscip. Top.* **1997**, *56*, 5705−5716.
(43) Si, L.; Massa, M. V.; Dalnoki-Veress, K.; Brown, H. R.; Jones, R. A. L. Chain Entanglement in Thin Freestanding Polymer Films. *Phys. Rev. Lett.* **2005**, *94*, 127801.
(44) Mundra, M. K.; Donthu, S. K.; Dravid, V. P.; Torkelson, J. M. Effect of Spatial Confinement on the Glass-Transition Temperature of Patterned Polymer Nanostructures. *Nano Lett.* **2007**, *7*, 713−718.
(45) Root, S. E.; Alkhadra, M. A.; Rodriquez, D.; Printz, A. D.; Lipomi, D. J. Measuring the Glass Transition Temperature of Conjugated Polymer Films with Ultraviolet−Visible Spectroscopy. *Chem. Mater.* **2017**, *29*, 2646−2654.
(46) Xie, R.; Lee, Y.; Aplan, M. P.; Caggiano, N. J.; Müller, C.; Colby, R. H.; Gomez, E. D. Glass Transition Temperature of Conjugated Polymers by Oscillatory Shear Rheometry. *Macromolecules* **2017**, *50*, 5146−5154.
(47) Stafford, C. M.; Harrison, C.; Beers, K. L.; Karim, A.; Amis, E. J.; VanLandingham, M. R.; Kim, H.-C.; Volksen, W.; Miller, R. D.; Simonyi, E. E. A buckling-based metrology for measuring the elastic moduli of polymeric thin films. *Nat. Mater.* **2004**, *3*, 545−550.
(48) Wu, H.-C.; Benight, S. J.; Chortos, A.; Lee, W.-Y.; Mei, J.; To, J. W. F.; Lu, C.; He, M.; Tok, J. B. H.; Chen, W.-C.; Bao, Z. A Rapid and Facile Soft Contact Lamination Method: Evaluation of Polymer Semiconductors for Stretchable Transistors. *Chem. Mater.* **2014**, *26*, 4544−4551.
(49) Wang, G.; Chu, P.-H.; Fu, B.; He, Z.; Kleinhenz, N.; Yuan, Z.; Mao, Y.; Wang, H.; Reichmanis, E. Conjugated Polymer Alignment: Synergisms Derived from Microfluidic Shear Design and UV Irradiation. *ACS Appl. Mater. Interfaces* **2016**, *8*, 24761−24772.
(50) Shaw, L.; Hayoz, P.; Diao, Y.; Reinspach, J. A.; To, J. W. F.; Toney, M. F.; Weitz, R. T.; Bao, Z. Direct Uniaxial Alignment of a Donor−Acceptor Semiconducting Polymer Using Single-Step Solution Shearing. *ACS Appl. Mater. Interfaces* **2016**, *8*, 9285−9296.
(51) Kleinhenz, N.; Persson, N.; Xue, Z.; Chu, P. H.; Wang, G.; Yuan, Z.; McBride, M. A.; Choi, D.; Grover, M. A.; Reichmanis, E. Ordering of Poly(3-hexylthiophene) in Solutions and Films: Effects of Fiber Length and Grain Boundaries on Anisotropy and Mobility. *Chem. Mater.* **2016**, *28*, 3905−3913.
(52) Poyraz, S.; Zhang, L.; Schroder, A.; Zhang, X. Ultrafast Microwave Welding/Reinforcing Approach at the Interface of Thermoplastic Materials. *ACS Appl. Mater. Interfaces* **2015**, *7*, 22469−22477.
(53) Huang, J.; Kaner, R. B. Flash welding of conducting polymer nanofibres. *Nat. Mater.* **2004**, *3*, 783−786.

DOI: 10.1021/acsapm.9b00321
ACS Appl. Polym. Mater. 2019, 1, 1778−1786